Geomechanics and Engineering, *Vol. 39, No. 4 (2024) 407-423*
https://doi.org/10.12989/gae.2024.39.4.407

Enhancing foundation bearing capacity in waterlogged ground for sustainable building construction

Mukhtiar Ali Soomro[1], Shaokai Xiong[1], Naeem Mangi*[1], Dildar Ali Mangnejo[3] and Sharafat Ali Darban[1]

[1]*School of Mechanics and Civil Engineering, China University of Mining and Technology, Xuzhou, Jiangsu, P.R. China*
[2]*School of Civil Engineering, Southwest Jiaotong University, Chengdu 610031, China*
[3]*Department of Civil Engineering, Mehran University of Engineering and Technology, Shaheed Zulfiqar Ali Bhutto Campus, Khairpur Mir's, Sindh, Pakistan*

(*Received January 17, 2024, Revised November 11, 2024, Accepted November 19, 2024*)

Abstract. Construction on waterlogged ground presents significant challenges for geotechnical engineers due to the low bearing capacity, high water table, and risks of post-construction settlement, all of which can compromise the stability of buildings. This study aims to investigate the settlement behavior of foundations on such terrains and recommend suitable foundation types to safely support building loads. To achieve these objectives, three-dimensional coupled consolidation analyses were performed to evaluate the bearing capacities of shallow footings with dimensions of 1.22 × 1.22 m² and 1.83 × 1.83 m². The results showed ultimate load capacities of approximately 10 kN and 21 kN, respectively, for these footings on waterlogged ground. To enhance these capacities, the use of pit sand as a filling material was explored, yielding substantial improvements. The bearing capacity of the 1.22 × 1.22 m² footing increased by a factor of 9, while the 1.83 × 1.83 m² footing saw a sixfold improvement. In addition, alternative foundation solutions were evaluated to achieve higher load-bearing capacities. These included raft foundations, single piles, pile groups, and piled raft foundations. Among these, a single pile demonstrated an ultimate load capacity of 300 kN, while a (2 × 2) pile group supported up to 400 kN. The piled raft foundation exhibited the highest capacity, with an ultimate load of 620 kN. These findings provide valuable insights into effective foundation designs for waterlogged conditions, enabling safer and more reliable construction practices.

Keywords: bearing capacity; coupled consolidation analysis; footings; waterlogged condition

1. Introduction

Construction on waterlogged ground has always been considered a challenging task by the civil engineering community. The high compressibility and low strength and are typical characteristics of such soils, making them inadequate to support the additional load of infrastructure built on them. Some additional considerations are required to provide a sufficiently strong foundation to support the development above ground. The foundation has to not only bear the dead and live loads without collapse, but also to undergo limited and uniform settlement with time (Salencon 2003). These types of soils are commonly found as extremely soft, unconsolidated deposits (Villalobos *et al.* 2003). Mahiyar and Patel (1997) did the research and recognized such types of soil as problematic materials for their low shear strength, high compressibility, and low permeability as well as considerable secondary compression or creep characteristics. Constructing large buildings over soft-soil sites can be challenging in an urban setting, as special care must be taken to ensure that primary consolidation and post-construction secondary settlements will not damage adjacent structures and utilities. In many instances, this means that methods to minimize the amount of settlement must be employed. This can be accomplished either by using a smaller loading condition or by altering the foundation conditions to withstand the required load (Alencar *et al.* 2019). Singh *et al*. (2007) found that in either case, the net goal is to reduce the potential settlements to an acceptable magnitude. If the shear stress in a mass of soil underneath a foundation exceeds the shear strength of the soil, the soil may then fail in shear, causing large settlements and resulting in a tilting or collapse of the structure. Shear failure takes place quickly as soon as the bearing capacity of the soil is exceeded, whereas consolidation settlements continue over a long period of years after the structure has been completed. As consolidation proceeds, more water is expelled from the soil. Thus, consolidation increases the shear strength of the soil with time (El Sawwaf and Nazer 2005, Bouassida *et al*. 2022, Rashid *et al.* 2020). The resistance to deformation of the soil depends upon factors like water content, bulk density, angle of internal friction and loading conditions. When excessive load is transmitted to the soil by a structural foundation, the settlement of the foundation takes place, which can endanger the stability of the structure (Ortiz 2001, Yang and Zhang 2017, Shirazi *et al*. 2020). The settlement due to load is caused basically on account of two factors: (i) the soil below footing gets compressed by certain amount, and (ii) since the foundations cover only a limited area, there is a possibility that the concentrated

*Corresponding author, Ph.D. candidate
E-mail: naeem08ce30@gmail.com

ISSN: 2005-307X (Print), 2092-6219 (Online)

stresses developed are so high as to cause actual rupture (shear failure) and displacement of soil below. In periods of wet weather, clay soils swell, and the cracks lend to close, the water deficiency developed in the previous dry periods may be partially replenished and a sub-surface zone or zones deficient in water may persist for many years. Leakage from water mains and underground sewers may also result in large volume changes. Therefore, special care must be taken to prevent such leakages (El Sawwaf and Nazer 2005, Lam 2010). Clay soils are seasonally affected by drying, shrinkage and cracking in dry and hot weather, and by swelling in the following wet weather to a depth which will vary according to the nature of the clay and the climatic condition of the region (El Sawwaf and Nazer 2005, Elam and Björdal 2020). The issue becomes more challenging when dealing with an expansive subgrade. Even if the flexible pavement is meticulously designed, the expansive nature of the subgrade introduces uncertainties that disrupt all predictions. It is a recognized fact that significant stresses can emerge during the volume change of a material, leading to manifestations such as cracking, heaving, and settlement in highway pavements. Consequently, road authorities are compelled to face substantial rises in the expenses associated with routine maintenance, rehabilitation, and even the reconstruction of deteriorated pavements, as highlighted by Hyunwook and William in 2009. When pavement structure, subjected to loads from trucks, is analyzed under different subgrade conditions – dry and saturated. The results reveal substantial vertical displacements in saturated drained and dry undrained subgrades, surpassing those in dry drained subgrade. Notably, vertical displacements under the shoulder's center are considerably lower than those occurring beneath various wheel loads, highlighting the differential effects based on subgrade conditions (Mostafa Deep Hashem 2013, Djellali *et al.* 2012). For most types of construction, water-logged ground is undesirable because of its low bearing capacity (Mohebkhah 2017). On sites liable to be water-logged in wet weather, it is desirable to determine the fluctuation of the water table in order to ascertain the directions of the natural drainage, and to obtain a clue to the design of intercepting drains to prevent the influx of groundwater on to the site from higher ground.

The seasonal variation in the level of water table should also be noted (El Sawwaf and Nazer 2005, Lee and Ng 2004). Increase in moisture extent results in substantial loss of bearing capacity in case of certain types of soils, which may lead to differential settlements (Al-Aghbari and Mohamedzein 2004). Specially repeated lowering and rising of water level in loose granular soils tend to compact the soil and cause settlement of the foundations. Prolonged lowering of the water table in fine-grained soils may introduce settlements because of the extrusion of water from the voids. Pumping water or draining water by wells or pipes from granular soils without adequate filter material as protection may, in a period of time, carry a sufficient number of fine particles away from the soil and cause settlement (El Sawwaf and Nazer 2005). All foundations settle under load. The critical factor is the differential settlement between the different parts of a structure itself. Excessive pressure is comparatively uncommon cause of settlement. Investigation of all layers under a foundation should be made as even thin layers, which are weak in shear, can cause settlement (Rajagopal *et al.* 1999). With structures built on sands and gravels the settlement is likely to be partially completed at the end of construction, but when the site is undertaken by clays or silts, settlement is likely to continue for a long time after construction and cracks may appear many years after completion. Due allowance shall, therefore, need to be made for this slow consolidation settlement (Dash *et al*. 2001, Bolton 1986).

As the soil settles, so does the foundation. The effect of settlement depends upon many factors such as its magnitude, uniformity, and the type of structure. If the contact pressure at the base of the footing on the soil is uniform, and uniformly distributed, settlements may be tolerable if the type of structure and/or its exploitation can withstand such settlements. However, a uniform, tolerable settlement should not be construed as a failure because settlement of a soil as a function of load is a normal physical phenomenon. The foundations of different elements of a structure may have un-equal settlements and the difference between such settlements will cause non-uniform or differential settlement, which may be disastrous, leading to cracking of the structural members, impairment of the structural rigidity of the building, and eventually to the collapse of the structure (Dash *et al.* 2003). It is known that the magnitude of the settlement depends not only on the compressibility of the soil, but also upon the size and shape of the footings of foundations, upon the stresses in the soil underneath the foundations, water regimen in the soil, and other factors. Compression of soil is manifested in settlement of foundations (El Sawwaf and Nazer 2005).

Whenever a deep excavation is made up to a large depth, the water table is encountered invariably. The water has to be pumped out so that workmen can work in dry condition in the excavated area. The lowering of water table by pumping seriously affects the structure founded in the vicinity. The effective pressure on the sub-soil increases due to lowering of water table. The increase of the effective pressure causes extra settlement of the nearby structures. In the case of sandy soil, the lowering of water table does not affect the structure so badly as in case of clayey soil. In case of clayey soil, the lowering of water table may cause settlements [El Sawwaf and Nazer 2005; Pirzada 2014).

The expulsion of water from the voids of the saturated clay soil by an externally applied load in the consolidation process, and the change in volume associated with such a process, are essentially a problem of permeability of a soil to water. The permeability, besides compressibility, is one of the principal factors relative to settlement of a soil, viz., and settlement of structure. The magnitude of settlement depends upon the compressibility of the soil, whereas the rate of consolidation depends on both permeability and compressibility (El Sawwaf and Nazer 2005). Permeability of soil is a very important physical property of soil because some of the major problems of soil and foundation engineering relate to it. It is well known that every soil mass has some voids and water tends to travel from one place to another through these voids (Chauhan *et al.* 2008,

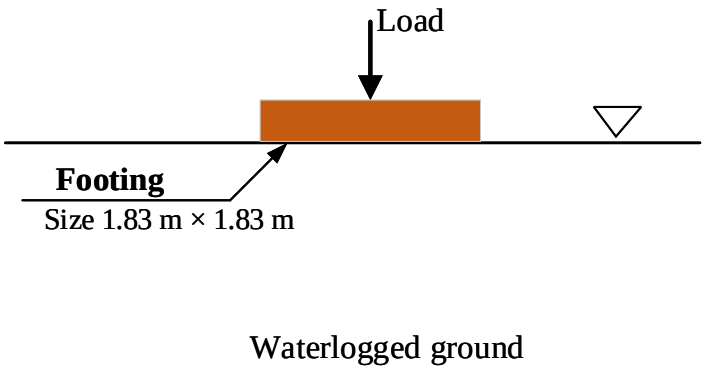

Fig. 1 Elevation view of the footing on the waterlogged ground

Afsharpour *et al*. 2022). In such type of waterlogged soils, it is very necessary to account for (i) the effect of ground water level on the stability of the foundation, (ii) foundation settlement' i.e., foundation failures, causes of foundation settlement, time-dependent settlement (iii) improvement of bearing capacity of soil through soil stabilizing methods, protection of excavation, safety of existing structure (El Sawwaf and Nazer 2005, Das *et al.* 2022, Hamza Gullu 2012, Ayman A. Abed 2008, Ottosen and Petersson 1992).

The problem statement based on the above literature review addresses the challenges posed by waterlogged ground, such as high compressibility and low shear strength, which make construction difficult due to low bearing capacity, high water table level, and potential post-construction and consolidation settlements that may damage buildings. The aim of the research is to understand the consolidation behavior of waterlogged soil. The specific objectives include determining the settlement behavior of the foundation and recommending suitable foundation types capable of safely sustaining building loads.

2. Three-dimensional finite element analysis

2.1 Description of geometry of the probelm studied

Firstly, the performance of shallow foundation was investigated in the waterlogged ground. Then the method to improve bearing capacity of the waterlogged ground was proposed and to support higher loads, different types of foundations such as raft, single pile, pile group and piled raft in waterlogged ground were suggested. To calculate and bearing capacity of the shallow foundation (footings) on waterlogged, three-dimensional coupled consolidation analyses were carried out using Abaqus software package. In Abaqus, the "Soils" step is used to simulate partially or fully saturated flow of single-phase fluid in porous media (Soomro *et al.* 2015, 2017). In this analysis type, an effective stress principle is used to describe the behaviour of the soil. The total stress tensor acting at a point in the soil, σ_{ij}, is composed of the pore fluid pressure p, as well as the effective stress σ'_{ij}.

$$\sigma_{ij}=\sigma'_{ij}+p\delta_{ij} \tag{1}$$

where δ_{ij} is the Kronecker delta.

In soils, the pore pressure is mainly caused by a "wetting liquid" pressure uw which is usually incompressible (water), as well as an average pressure stress in the other fluid (air) ua which is usually compressible.

$$p=\chi u_w+(1-\chi) \tag{2}$$

where χ denotes a factor that depends on saturation and tension on the surface of the liquid or solid. Darcy's law is adopted to describe the water flow through the soil [14]

$$(nV^f - V^s) = k\cdot(-\nabla_x p + \rho_f(f-\gamma^f - a)) \tag{3}$$

where k is the anisotropic permeability tensor, and a is the dynamic tortuosity vector. V^f and V^s stand for the velocity fields of fluid and skeleton, respectively. n is the Eulerian porosity. f refers to the body force density per mass unit, and γ^f is the fluid acceleration vector.

The bearing capacities of three sizes of footings (1.83 m × 1.83 m, 1.22 m × 1.22 m) on waterlogged and improved ground (pit sand as fill material) were determined. Fig. 1 shows the elevation view of the configuration of numerical load test for a footing of typical size of 1.83 m × 1.83 m on the waterlogged ground. The depth of the all the footing were taken as 0.75 m.

2.2 Improvement of bearing capacity by filling materail (pit sand)

Fig. 2 shows the footing of size 1.83 m × 1.83 m placed on the filling material (i.e., pit sand) on the waterlogged ground. The depth of pit sand was 1.5 m. The behaviour of pit sand was modelled by linear elastic perfectly plastic model with Mohr-Coulomb failure criterion was used to capture soil behaviour. Pit sand, with its granular structure, enhanced the shear strength of the foundation soil. This improvement resulted from the replacement of weaker, saturated soil with a more stable material capable of resisting deformation under load. By replacing the waterlogged soil, the pit sand reduced excess pore water

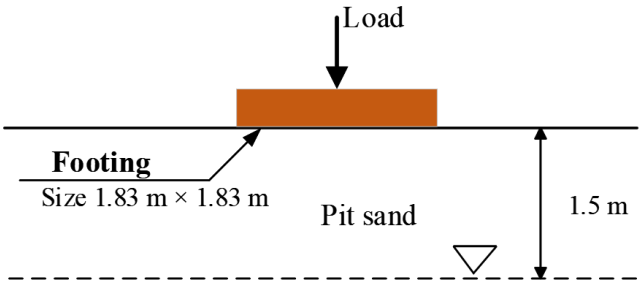

Fig. 2 Elevation view of the footing on the pit sand

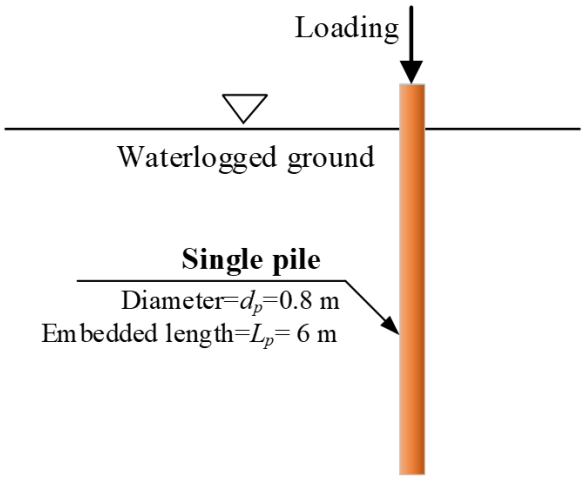

Fig. 3 Elevation view of the single pile in the waterlogged ground

Table 1 Improved parameters

Parameters	Values
Young's Modulus (MN/m^2)	30
Poisson's ratio	0.2
Dry unit weight (kN/m^3)	17.0
Saturated unit weight (kN/m^3)	19.0
Cohesion (c')	1.0
Friction angle (ϕ')	31
Permeability (m/day)	0.2

pressure, which typically undermines the load-bearing capacity of soil. This reduction helped the footing to maintain stability under applied loads. Moreover, the compacted pit sand acted as an intermediary layer, distributing the load more uniformly to the underlying soil. This reduced localized stresses and prevented excessive settlement or instability of the footings. In addition, Pit sand's permeability facilitated drainage in the waterlogged area, reducing the potential for further saturation and providing long-term stability. These mechanisms worked collectively to achieve the notable improvements in bearing capacity observed in the study. The findings highlight the importance of appropriate material selection and placement techniques in mitigating the challenges posed by waterlogged conditions.

The sand parameters are summarized in Table 1.

2.3 Proposed alternative types of foundations with higher bearing capacity

In addition to filling material, alternative to shallow foundations (i.e., (1.22×1.22 m^2), (1.83×1.83 m^2) footings) are proposed. The proposed foundation types are raft, single pile, (2×2) pile group and piled raft on waterlogged ground. Fig. 3 shows the elevation view of geometry of single pile.

The diameter and embedded depth of the pile was taken as 0.8 m and 6 m, respectively. Eight-noded hexahedral brick elements were used to model the pile (Soomro *et al.* 2020).

Fig. 4 shows the elevation view of geometry of (2×2) pile group. The diameter and embedded depth of each pile was taken as 0.8 m and 6 m, respectively. All the four piles related to a 0.5 m thick pile cap. Fig. 5 shows the elevation

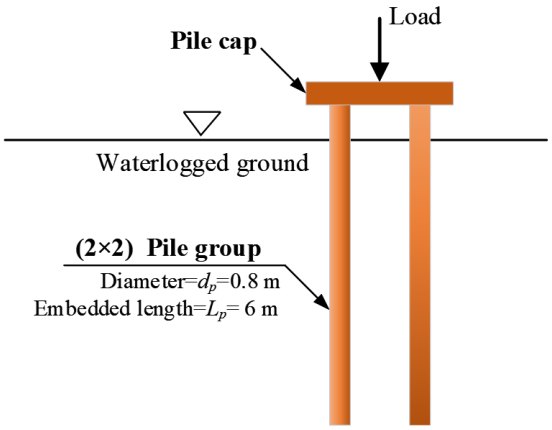

Fig. 4 Elevation view of the (2×2) pile group in the waterlogged ground

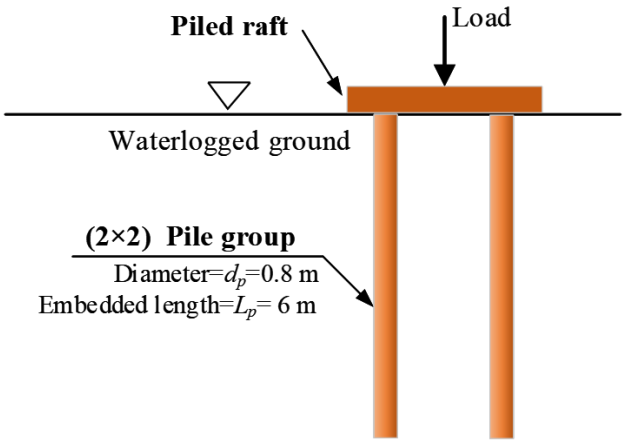

Fig. 5 Elevation view of the piled raft in the waterlogged ground

view of geometry of piled raft. The diameter and embedded depth of each pile was taken as 0.8 m and 6 m, respectively. All the four piles related to 0.7 m thick raft which is resting on the ground.

2.4 Constitutive model and its parameters

The modified Cam-clay model was employed to simulate soil behavior. This elastoplastic model incorporates incremental hardening and softening, with nonlinear elasticity and the hardening/softening response controlled by volumetric plastic strain. It has been effectively utilized to replicate the behavior of soft soils, as demonstrated in the works of Roscoe and Burland (1968) and Wood (1991). Theoretically, the model's formulation is grounded in elasticity, plasticity, and critical-state principles, making it well-suited for accurately capturing volume changes under various loading conditions, as well as representing nonlinear behavior, softening and hardening phenomena, and the critical state. Table 2 summarizes the parameters of modified cam clay model for waterlogged ground. The concrete footings, piles, raft and pile are assumed linear elastic with Young's modulus of 35 GPa and Poisson's ratio of 0.25 (Soomro *et al.* 2023a, b). In order to consider the interaction between soil and structures,

Table 2 Modified cam clay model parameters

Description	Parameters
Effective angle of shearing resistance at critical state: ϕ'	29.5°
The slope of the critical state line in p'-q space; M	1.18
The slope of the isotropic normal compression line in the e -lnp' plane, λ	0.103
The slope of unloading reloading line in the e - lnp' plane, κ	0.015
The specific volume of normal compression line at unit pressure, N	1.31
Dry density (kg/m^3)	1558
Initial void ratio (e)	0.7
Coefficient of permeability, k (m/s)	9.26×10^{-6}

specific properties related to tangential behaviour and normal behaviour are chosen for the contact between the battered piles and soil. The Coulomb Friction model is utilized to define frictional contact properties, enabling the simulation of tangential behaviour. On the other hand, the Hard Contact model is employed to replicate the nature of surface contact and simulate normal behaviour in Abaqus.

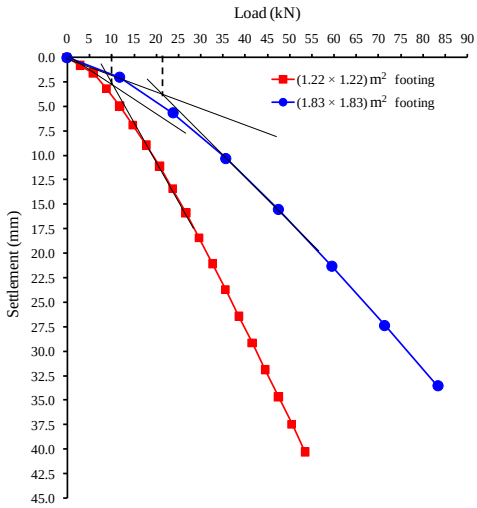

Fig. 6 Load settlement curve for footings on the waterlogged ground

A limiting shear displacement of 5 mm was assumed to achieve full mobilization of the interface friction equal to $\mu \times p'$, where p' is the normal effective stress between two contact surfaces, and a typical value of μ for a bored pile of 0.35 was used in all analyses (Soomro *et al*. 2024a, b). Mayne and Kulhawy's Eq. (1) (Mayne and Kulhawy 1982), was used to calculate lateral earth pressure coefficient at rest K_o. The coefficient of lateral earth pressure at rest, is estimated by

$$K_0 = (1 - sin\varphi')(OCR)^{sin\varphi'} \quad (4)$$

2.5 Numerical modelling procedure

The numerical modelling procedure of the load test of footing in the waterlogged ground is summarized as follows

1. Generate the geostatic stresses at K_0 value in the mesh for each case
2. Activate the elements of the footing
3. The footing was loaded incrementally with each increment of 3 kN up to maximum 60 kN over a period of 24 hours

2.6 Ultımate bearıng capacıty of the footıngs restıng on waterlogged ground

Fig. 6 shows the relationship between load and settlement for each of the two different sizes of footings (i.e. 1.22 ×1.22 m^2, 1.83×1.83 m^2) resting on the waterlogged ground. These load settlement relationships were obtained from the numerical load test carried out for the footings founded on the waterlogged ground. The ultimate load carrying capacity is obtained from load relationship based on the estimated yield point (which is defined as the load-settlement curve starts to deviate from the tangent line) method. The estimated load "yield point" is also shown in the figure.

It can be seen from the figure that the load settlement curves for each footing exhibit linear behaviour in the beginning. However, with further increment of load, non-linear characteristics of the curves were observed with a distinctive "yield" point. As the footing size increases, the yield point becomes higher. The response of bigger size footing was stiffer than that of smaller size footing. To be more specific, for a given load the larger size footing settles less than the smaller size footing. Using tangent intersection method, the computed ultimate load for the footing of sizes (1.22×1.22 m^2) and (1.83×1.83 m^2) were estimated to be 10 kN and 21 kN, respectively. Using load settlement curves, the settlement of footings of sizes (1.22×1.22 m^2) and (1.83×1.83 m^2) due to their corresponding calculated ultimate loads were determined as 2.5 mm and 3.5 mm, respectively. In addition, the computed bearing capacity was compared with that calculated obtained from analytical solution given by (Meyerhof 1963). It was observed that calculated bearing capacity of the both the footings was smaller than that of calculated. This is because in analytical solution given by Meyerhof (1963) assumed that soil behave as perfectly plastic. In contrast, the soil behaviour modeled in this numerical analysis is assumed as elasto-plastic material with hardening. The soil will deform due to loading as well as yield progressively because of finite element formulation. The ultimate load calculated from Meyerhof's equations for each of the three footings of sizes (1.22×1.22 m^2) and (1.83×1.83 m^2) were 15 kN and 28 kN, respectively. The obtained bearing capacity of the footings founded on the waterlogged ground is quite low. Therefore, it is desirable that bearing capacity of the waterlogged ground should be improved or alternative foundation types (which has higher bearing capacity) can be suggested.

3. Results and discussion

3.1 Methods to ımprove load carryıng capacıty of footıngs

3.1.1 Improved ultimate bearing capacity of footing size (1.22×1.22) m^2

Fig. 7 shows the load versus settlement curves for the footing of size (1.22×1.22) m^2 resting on the pit sand used as filling material over waterlogged ground. For comparison, the

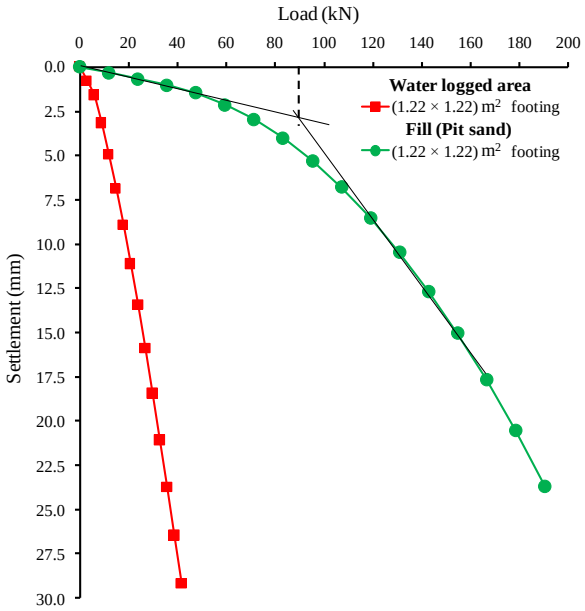

Fig. 7 Load settlement for the footing of size (1.22×1.22) m^2 founded on the pit sand over waterlogged ground

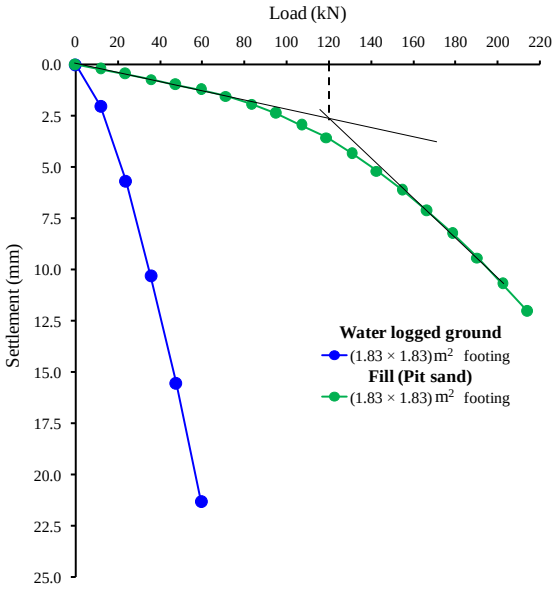

Fig. 8 Load settlement for the footing of size (1.83×1.83) m^2 founded on the pit sand over waterlogged ground

load settlement curve obtained from the load test of the footing founded on waterlogged ground is also included in the figure. Owing to higher stiffness of the pit sand than that of the waterlogged clay, the response of load settlement curve was found to be quite stiff. To be more specific, at a given load the settlement of footing on the pit sand was smaller than that on waterlogged ground. Using tangent intersection method, the computed ultimate load for the footing was estimated to be 90 kN (62.5 kPa). This means that the bearing capacity of the footing is increased 9 times of that bearing capacity on waterlogged ground. With factor of safety of 1.5, the working loads were determined as 60 kN. Using load settlement curves, the settlement of footing due to their corresponding computed ultimate load was obtained as 2.5 mm.

3.1.2 Improved ultimate bearing capacity of footing size (1.83×1.83) m^2

Fig. 8 shows the load versus settlement curves for the footing of size (1.83×1.83) m^2 resting on the pit sand used as filling material over waterlogged ground. For comparison, the load settlement curve obtained from the load test of the footing founded on waterlogged ground is also included in the figure. Owing to higher stiffness of the pit sand than that of the waterlogged clay, the response of load settlement curve was found to be quite stiff. To be more specific, at a given load the settlement of footing on the pit sand was smaller than that on waterlogged ground. Using tangent intersection method, the computed ultimate load for the footing was estimated to be 120 kN (80 kPa). This means that the bearing capacity of the footing is increased 6 times of that bearing capacity on

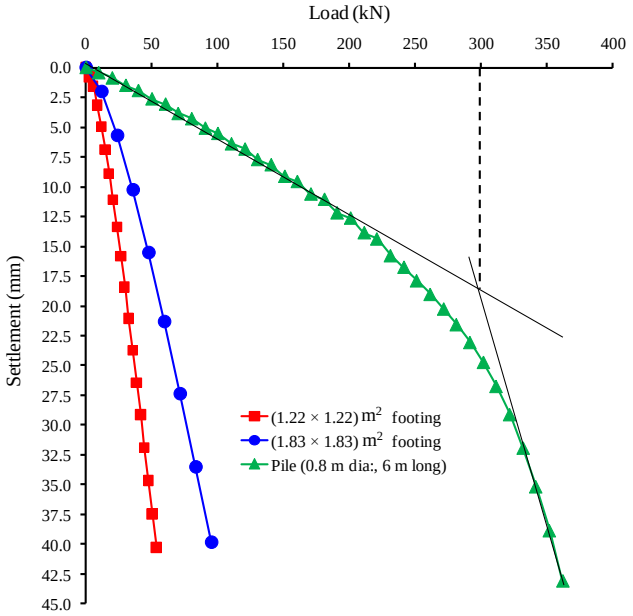

Fig. 9 Computed load settlement curve for single pile founded in the waterlogged ground

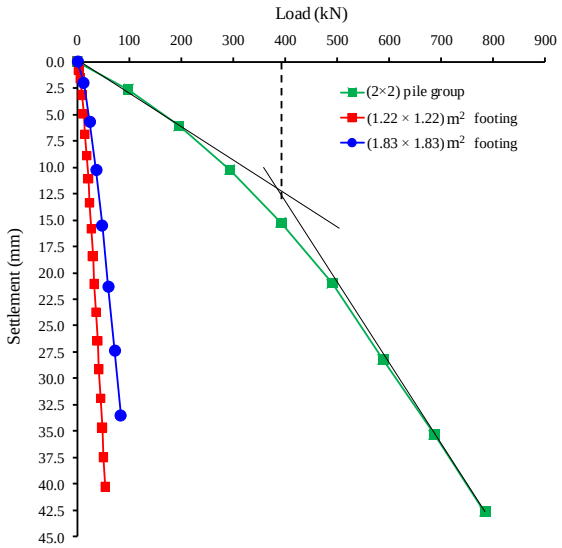

Fig. 10 Computed load settlement relationship for (2×2) pile group founded in the waterlogged

waterlogged ground. With factor of safety of 1.5, the working loads were determined as 80 kN. Using load settlement curves, the settlement of footing due to their corresponding computed ultimate load was obtained as 2.5 mm.

3.2 Proposed alternative types of foundations with higher bearing capacity

3.2.1 Ultimate load carrying capacity of a single pile in waterlogged ground

Fig. 9 illustrates the load settlement relationship obtained from a numerical pile load test. For comparison, the load settlement curves from load test performed on shallow footings with sizes (1.22×1.22) m^2 and (1.83×1.83) m^2 are included in the figure.

3.2.2 Ultimate load carrying capacity of a (2×2) pile group in waterlogged ground

Fig. 10 shows the load settlement relationship obtained from a numerical load test of the (2×2) pile group. For comparison, the load settlement curves from load test performed on shallow footings with sizes (1.22×1.22) m^2 and (1.83×1.83) m^2 and single pile are included in the figure. It can be seen that the load settlement curve for (2×2) pile group exhibits stiffer behaviour than that of the single pile and the footings. Initially, the load settlement curve for single pile exhibits linear behaviour. However, with further increment of load, non-linear characteristics of the curves were observed with a distinctive "yield" point. Using tangent intersection method, the ultimate load carrying capacity of (2×2) pile group was computed as 620 kN which is significantly higher than

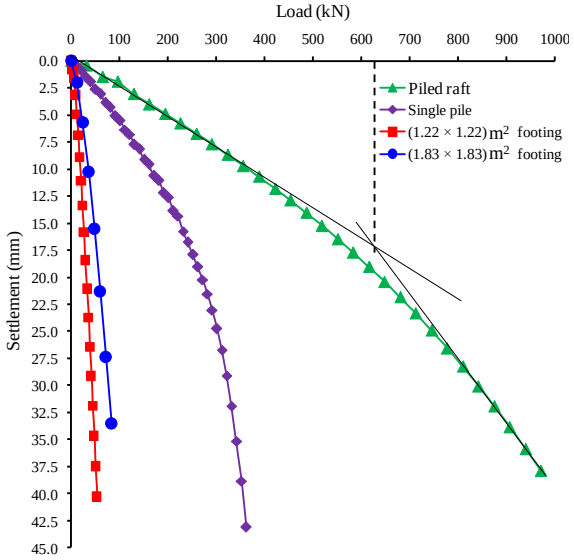

Fig. 11 Computed load settlement relationship for piled raft founded in the waterlogged

that of single pile and footings. With factor of safety of 1.5, the working loads were determined as 413 kN. Using load settlement curves, the settlement of footing due to their corresponding computed working load was obtained as 11 mm.

It can be seen that the response of load settlement curves of single pile is much stiffer than that of the footings. Initially, the load settlement curve for single pile exhibits linear behaviour. However, with further increment of load, non-linear characteristics of the curves were observed with a distinctive "yield" point. Using tangent intersection method, the ultimate load carrying capacity of single pile was computed as 300 kN which is significantly higher than that of shallow footings. With factor of safety of 1.5, the working loads were determined as 200 kN. Using load settlement curves, the settlement of footing due to their corresponding computed working load was obtained as 12.5 mm.

3.2.3 Ultimate load carrying capacity of a piled raft in waterlogged ground

Fig. 11 shows the load settlement relationship obtained from a numerical load test of the piled raft. For comparison, the load settlement curves from load test performed on shallow footings with sizes (1.22×1.22) m^2 and (1.83×1.83) m^2 are included in the figure. It can be seen that the load settlement curve for piled raft exhibits stiffer behaviour than that of the single pile and the footings. Initially, the load settlement curve for single pile exhibits linear behaviour. However, with further increment of load, non-linear characteristics of the curves were observed with a distinctive "yield" point. Using tangent intersection method, the ultimate load carrying capacity of piled raft was computed as 400 kN which is significantly higher than that of single pile and footings. With factor of safety of 1.5, the working loads were determined as 267 kN. Using load settlement curves, the settlement of footing due to their corresponding computed working load was obtained as 10 mm.

3.3 Performance of the different types of foundations during construction of two storey framed building

3.3.1 Settlement of shallow foundation in water logged ground due to loading of two storey building

Fig. 12 shows the settlements of the footing sizes (1.22×1.22) m^2 and (1.83×1.83) m^2 due to construction of different structural components (i.e., foundation, plinth beams, floor, GF columns, GF beams, GF roof, FF columns, FF beams and FF roof) of the two-storey building. In addition to settlement due to dead weight of the structural components, settlement due to application of live loads on floor, ground floor roof and first floor roof is included in the figure.

It can be seen from the figure settlement increase with construction of each structural components and application of live load on floor and roofs. The settlement of the footing size (1.83×1.83) m^2 during construction of each structural component of the building is smaller than that of footing size (1.22×1.22) m^2. This is because of stiffer load settlement behavior. The total settlements of footing size (1.83×1.83) m^2 and (1.22×1.22) m^2 due dead and love load are 135 mm and 208, respectively. The settlement of the footing of size (1.22×1.22) m^2 54% was higher than that of (1.83×1.83) m^2. However, the settlement of footing of size is still much larger than required settlement of the building.

Figs. 13(a) and 13(b) show the displacements contours of settlement of soil and the building due to self-load of the building and live loads for the footing sizes (1.22×1.22) m^2 and (1.83×1.83) m^2, respectively. It helps to visualize the displacement of each component of the building and the soil movement due to the loadings.

3.3.2 Settlement of raft foundation in water logged ground due to loading of two storey building

Fig. 14 shows the settlements of the raft foundation due to construction of different structural components (i.e. foundation, plinth beams, floor, GF columns, GF beams, GF roof, FF columns, FF beams and FF roof) of the two-storey building. In addition to settlement due to dead weight of the structural components, settlement due to application of live loads on

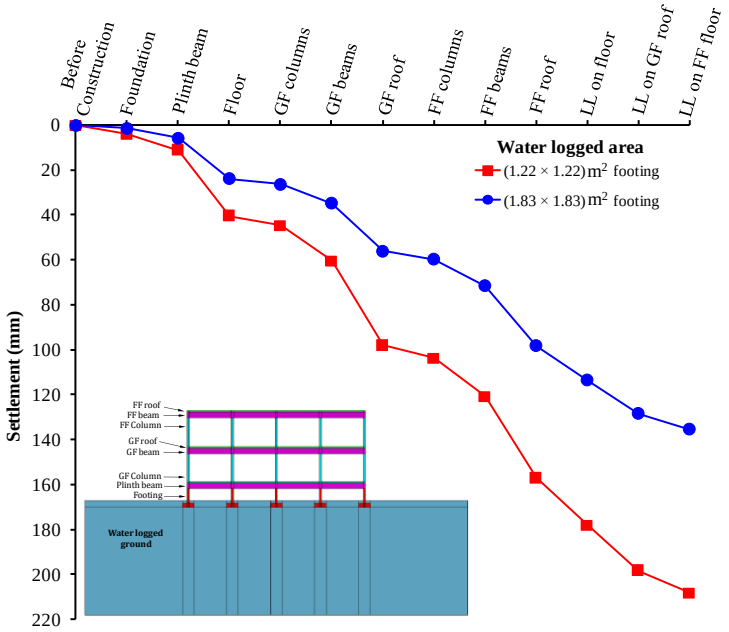

Fig. 12 Settlement of shallow foundations in waterlogged ground due to dead load of structural components and live loads the floor and roofs

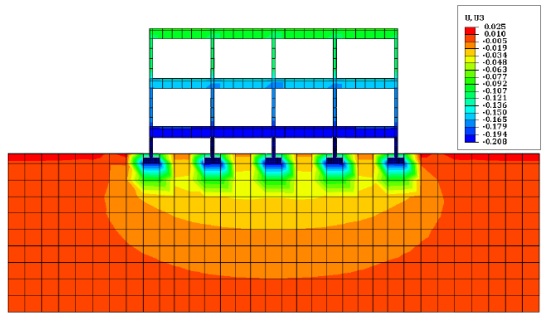

(a)

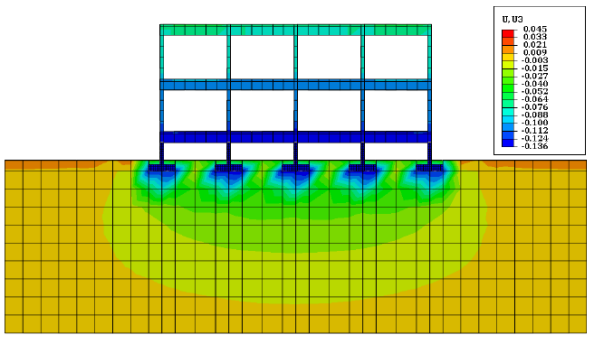

(b)

Fig. 13 Displacement contours after construction of the building and application of live loads (a) (1.22×1.22) m^2 (b) (1.83×1.83) m^2

floor, ground floor roof and first floor roof is included in the figure. For comparison, settlements of the footing sizes (1.22×1.22) m^2 and (1.83×1.83) m^2 are included in the figure.

It can be seen from the figure settlement increase with construction of each structural components and application of live load on floor and roofs. The settlement of the raft during construction of each structural component of the building is smaller than that of footing size (1.22×1.22) m^2 and (1.83×1.83) m^2. This is because of stiffer response of the raft to loading. The reduction in settlement for the footing size (1.83×1.83) m^2 and (1.22×1.22) m^2 are 37% and 59%, respectively. The total settlement of raft is 85 mm. Figs. 15 shows the displacements contours of settlement of soil and the building due to self-load of the building and live loads for the

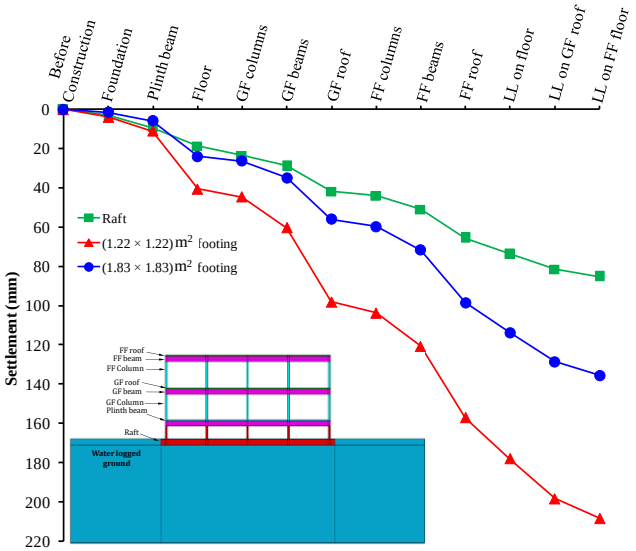

Fig. 14 Load settlement for the footing of size (1.22×1.83) m^2 founded on improved ground

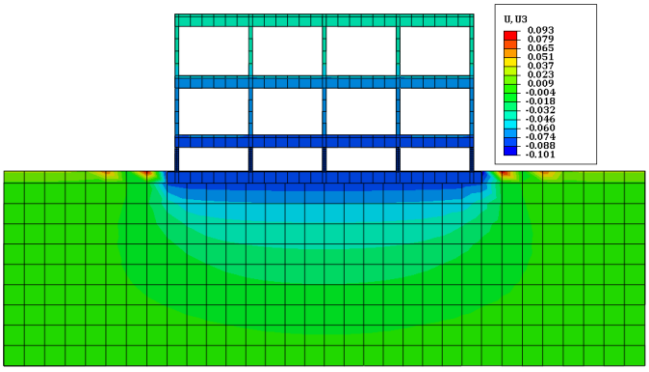

Fig. 15 Displacements contours of settlement of soil and the building for raft foundation

raft foundation. It helps to visualize the displacement of each component of the building and the soil movement due to the loadings.

3.3.3 Settlement of shallow foundation on pit sand over water logged ground due to loading of two storey building

Fig. 16 shows the settlements of the footing sizes (1.22×1.22) m^2 and (1.83×1.83) m^2 on pit sand over waterlogged ground due to construction of different structural components (i.e., foundation, plinth beams, floor, GF columns, GF beams, GF roof, FF columns, FF beams and FF roof) of the two-storey building. In addition to settlement due to dead weight of the structural components, settlement due to application of live loads on floor, ground floor roof and first floor roof is included in the figure.

It can be seen from the figure settlement increase with construction of each structural components and application of live load on floor and roofs. Comparing to settlement of both footings on waterlogged area (see Fig. 12), the footings on pit sand settled much smaller. This is because of higher stiffness of the pit sand than that of waterlogged clay. The reduction in settlement for the footing size (1.83×1.83) m^2 and (1.22×1.22) m^2 are 84% and 82%, respectively. Furthermore, the settlement of the footing size (1.83×1.83) m^2 during construction of each structural component of the building is smaller than that of footing size (1.22×1.22) m^2. This is because of stiffer load settlement behavior. The total settlements of footing size (1.83×1.83) m^2 and (1.22×1.22) m^2 due dead and live load are 21 mm and 36 mm, respectively. The settlement of the footing of size (1.22×1.22) m^2 42% was higher than that of (1.83×1.83) m^2. However, the settlement of footing of size is still much larger than required settlement of the building. Figs. 17 (a) and 17(b) show the displacements contours of settlement of soil and the building due to self-load of the building and live loads for the footing sizes (1.22×1.22) m^2 and (1.83×1.83) m^2, respectively. It helps to visualize the displacement of each component of the building and the soil movement due to the loadings.

3.3.4 Settlement of single piles in water logged ground due to loading of two storey building

Fig. 18 shows the settlements of the single piles of different lengths (i.e. Lp = 6 m, 10 m and 15 m) with diameter dp = 0.8 m in waterlogged ground due to construction of different structural components (i.e., foundation, plinth beams, floor, GF

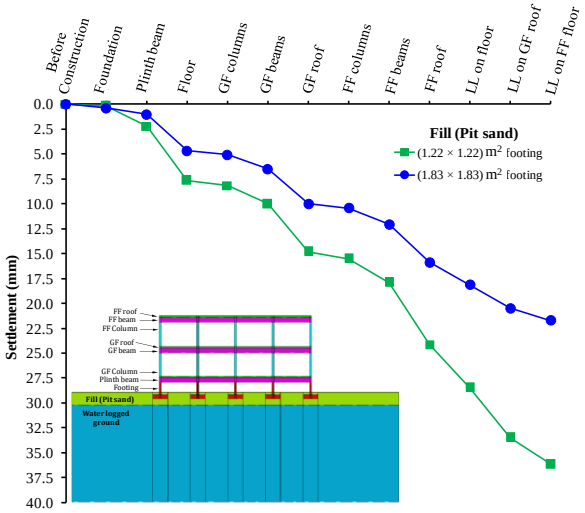

Fig. 16 Settlement of shallow foundations on pit sand due to dead load of structural components and live loads the floor and roofs

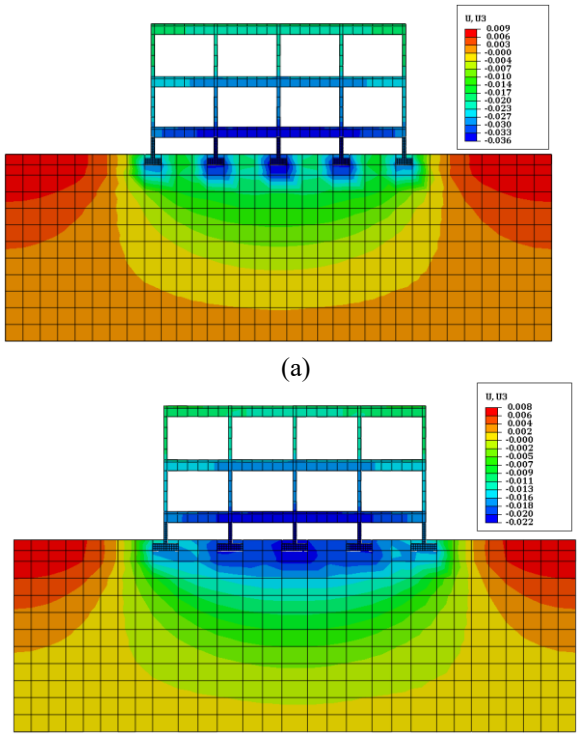

(a)

(b)

Fig. 17 Displacement contours after construction of the building and application of live loads (a) (1.22×1.22) m^2 and (b) (1.83×1.83) m^2

columns, GF beams, GF roof, FF columns, FF beams and FF roof) of the two-storey building.

In addition to settlement due to dead weight of the structural components, settlement due to application of live loads on floor, ground floor roof and first floor roof is included in the figure. It can be seen from the figure settlement increase with construction of each structural components and application of live load on floor and roofs. Comparing to settlement of the footing size (1.83×1.83) m^2 and (1.22×1.22) m^2 in waterlogged ground and pit sand (see Figs. 12 and 13), the settlements of the pile with lengths of 10 m and 15 m are much smaller. This is because of the pile carries the load with help of shaft and end-bearing resistance. It transfers the load in deeper ground which is stiffer than the ground surface. The reduction in settlement for the piles of lengths 10 m and 15 m are 55% and 72%, respectively. Moreover, the settlement of the pile with larger length is smaller than that of smaller length.

The total settlements of single piles with length Lp = 6 m, 10 m and 15 m due dead and live load are 54 mm, 24 mm, and 15 mm, respectively.

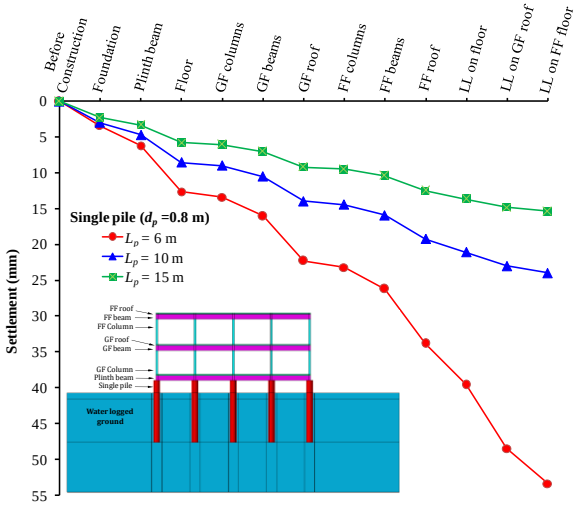

Fig. 18 Settlement of single piles (Lp = 6 m, 10 m and 15 m) due to dead load of structural components and live loads the floor and roofs

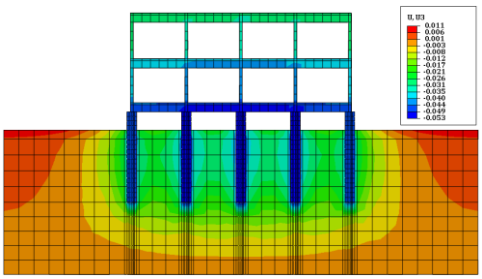

(a)

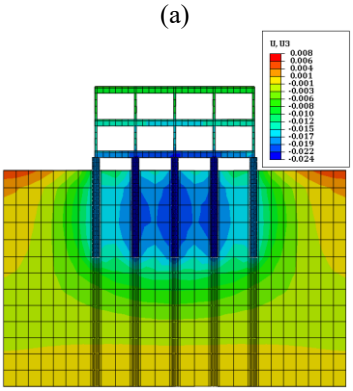

(b)

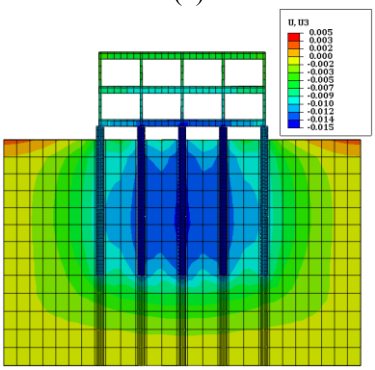

(c)

Fig. 19 Displacement contours after construction of the building and application of live loads on single pile of lengths (a) *Lp* = 6 m, (b) *Lp* = 10 m and (c) L*p* = 15 m

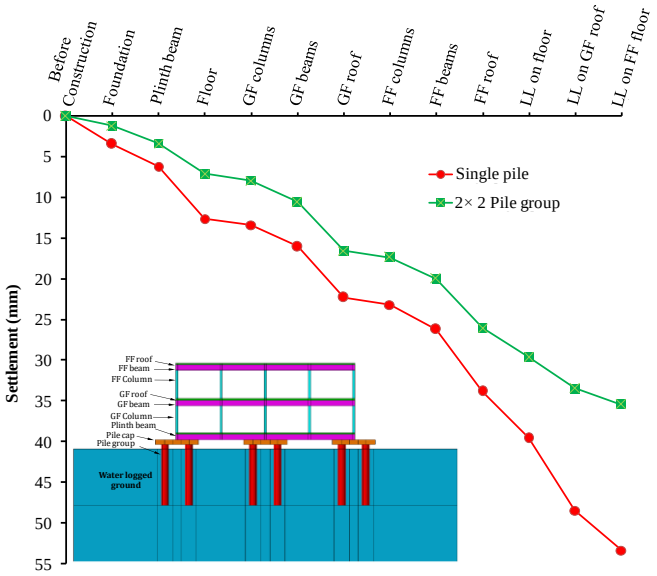

Fig. 20 Settlement of the (2×2) pile group due to dead load of structural components and live loads the floor and roofs

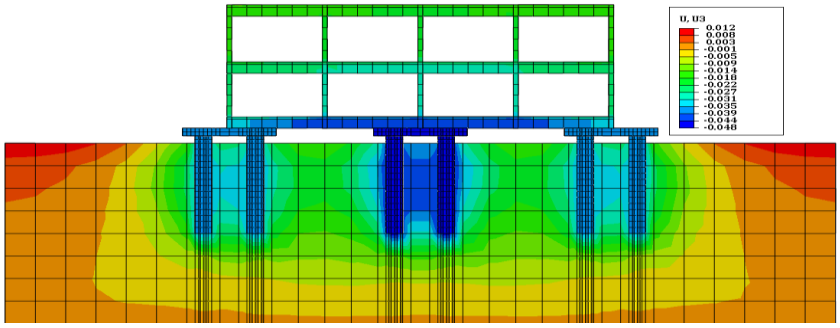

Fig. 21 Displacement contours after construction of the building and application of live loads on pile groups

Figs. 19(a)-19(c) show the displacements contours of settlement of soil and the building due to self-load of the building and live loads for the pile lengths Lp = 6 m, 10 m and 15 m, respectively. It helps to visualize the displacement of each component of the building and the soil movement due to the loadings.

3.3.5 Settlement of (2×2) pile group in water logged ground due to loading of two storey building

An alternative to increase pile length, (2×2) pile group with length of each pile *Lp* = 6 m and diameter *dp* = 0.8 m is proposed. Fig. 20 shows the settlements of the pile group in waterlogged ground due to construction of different structural components (i.e., foundation, plinth beams, floor, GF columns, GF beams, GF roof, FF columns, FF beams and FF roof) of the two-storey building.

In addition to settlement due to dead weight of the structural components, settlement due to application of live loads on floor, ground floor roof and first floor roof is included in the figure. For comparison, settlement of single pile with *Lp* = 6 m and *dp* = 0.8 m is included in the figure.

It can be seen from the figure settlement increase with construction of each structural components and application of live load on floor and roofs. Comparing to settlement of the single pile, the settlements of the pile group with length is smaller. This is because of the pile group response to loading is stiffer than that of the single pile. It transfers the load in deeper ground which is stiffer than the ground surface. The reduction in settlement for the pile group is 35%. The total settlement of the pile group due dead and live load is 35 mm.

Fig. 21 shows the displacements contours of settlement of soil and the building due to self-load of the building and live loads for the (2×2) pile group. It helps to visualize the displacement of each component of the building and the soil movement due to the loadings.

3.3.6 Settlement of the piled raft in water logged ground due to loading of two storey building

Fig. 22 shows the settlements of the piled raft with 9 and 13 numbers of piles (L*p* =6 m and d*p* = 0.8 m) in waterlogged ground due to construction of different structural components (i.e. foundation, plinth beams, floor, GF columns, GF beams, GF roof, FF columns, FF beams and FF roof) of the two-storey building.

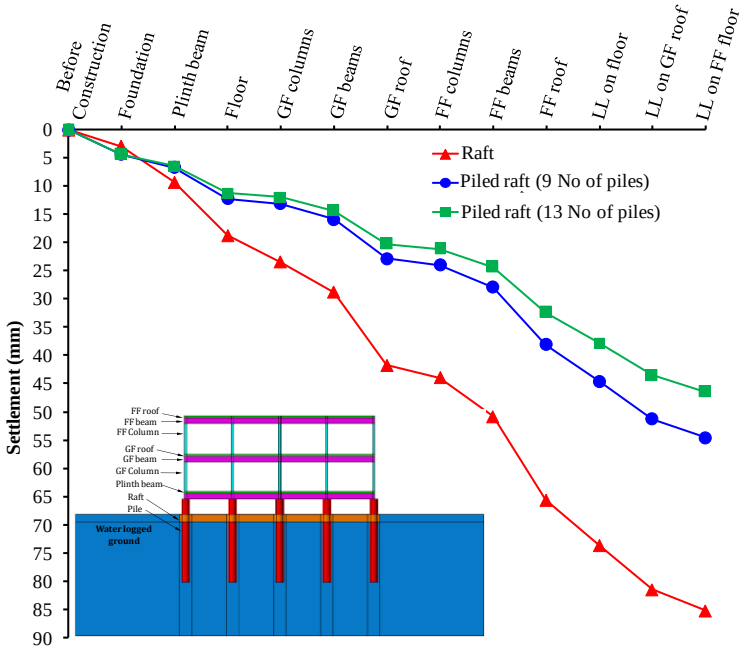

Fig. 22 Settlement of the piled raft with 9 and 13 number of piles due to dead load of structural components and live loads the floor and roofs

In addition to settlement due to dead weight of the structural components, settlement due to application of live loads on floor, ground floor roof and first floor roof is included in the figure. For comparison, settlement of the raft is included in the figure. It can be seen from the figure settlement increase with construction of each structural components and application of live load on floor and roofs. Comparing to settlement of the raft, the settlements of the piled foundation with 9 and 13 numbers of piles is smaller. This is because the piles underneath the raft. The piles transfer the load of superstructure to deeper layers of the waterlogged ground. The total settlement of the piled raft due dead and live load is 46 mm. However, the settlement of footing of size is still much larger than required settlement of the building.

4. Conclusions

The paper aims to examine foundation settlement behavior and recommend suitable types. It conducted analyses on shallow footings, finding low ultimate load capacities, and explored the use of filling material to enhance bearing capacity. Additionally, alternative foundation types such as single piles, pile groups, and piled rafts were proposed. Based on the ground conditions and geometry, the following conclusions can be drawn.

- The computed ultimate load for the footing of sizes (1.22×1.22 m^2), (1.83×1.83 m^2) on waterlogged area were estimated to be 10 kN and 21 kN, respectively. The settlements due to the ultimate loads for the footing of sizes (1.22×1.22 m^2), (1.83×1.83 m^2) were determined as 2.5 mm and 3.5 mm, respectively.
- The bearing capacity of the footing can be improved by filling material (i.e., pit sand) on waterlogged areas. The bearing capacity of the footing of sizes (1.22×1.22 m^2), (1.83×1.83 m^2) on pit sand increased by 800% and 500%, respectively.
- Alternative types of the foundations in the waterlogged ground were suggested to get higher bearing capacity. The types of foundations are raft, single pile, pile group and piled raft.
- The ultimate load carrying capacity of single pile was computed as 300 kN which is significantly higher than that of shallow footings.
- The ultimate load carrying capacity of (2×2) pile group was computed as 400 kN. With factor of safety of 1.5, the working loads were determined as 267 kN. Using load settlement curves, the settlement of footing due to their corresponding computed working load was obtained as 10 mm.
- The ultimate load carrying capacity of piled raft was computed as 620 kN which is significantly higher than that of single pile and footings. With factor of safety of 1.5, the working loads were determined as 413 kN. Using load settlement curves, the settlement of footing due to their corresponding computed working load was obtained as 11 mm.

Acknowledgments

The authors would like to acknowledge the financial support provided China University of Mining and Technology, Xuzhou, China.

References

Abed, A.A. (2008), "Numerical modeling of expansive soil behavior", Ph.D thesis, Institute for geotechnical, Stuttgart University, Germany.

Afsharpour, S., Payan, M., Chenari, R.J., Ahmadi, H. and Fathipour, H. (2022), "Bearing capacity of strip footings on unsaturated soils under combined loading using LEM", *Geomech. Eng.*, **31**(2), 223-235. https://doi.org/10.12989/gae.2022.31.2.223.

Al-Aghbari, M.Y. and Mohamedzein, Y.E.A. (2004), "Bearing capacity of strip foundations with structural skirts", *J. Geotech. Geol. Eng.*, **22**(1), 43-57. https://doi.org/10.1023/B:GEGE.0000013997.79473.e0.

Amin, M. (2017), "Bearing capacity of strip footings on a stone masonry trench in clay", *Geomech. Eng.*, **13**(2), 255-267. https://doi.org/10.12989/gae.2017.13.2.255.

Bolton, M.D. (1986), "The strength and dilatancy of sands", *Geotechnique*, **36**(1), 65-78.

Bouassida, M., Fattah, M.Y. and Mezni, N. (2022), "Bearing capacity of foundation on soil reinforced by deep mixing columns", *Geomech. Geoeng.*, **17**(1), 309-320. https://doi.org/10.1080/17486025.2020.1755458.

Chauhan, M.S., Mittal, S. and Mohanty, B. (2008), "Performance evaluation of silty sand sub-grade reinforced with fly ash and fiber", India.

Das, S., Halder, K. and Chakraborty, D. (2022), "Seismic bearing capacity of shallow embedded strip footing on rock slopes", *Geomech. Eng.*, **30**(2), 123-138. https://doi.org/10.12989/gae.2022.30.2.123.

Dash, S.K., Krishnaswamy, N. and Rajagopal, K, (2001), "Bearing capacity of strip footing supported on geocell-reinforced sand", *Geotext. Geomembranes*, **19**(4), 235-256. https://doi.org/10.1016/S0266-1144(01)00006-1.

Dash, S.K., Sireesh, S. and Sitharam, T.G. (2003), "Behavior of geocell reinforced sand beds under circular footing", *Ground Improvement,* **7**, 111-115. https://doi.org/10.1680/grim.2003.7.3.111.

Djellali, A., Ounis, A. and Saghafi, B. (2012), "Behavior of flexible pavements on expansive soils", *J. Transport. Eng.*, **1**(1), 1-14.

El Sawwaf, M.E.I. and Nazer, A. (2005), "Behavior of circular footings on confined granular soil", *J. Geotech. Geoenviron. Eng.- ASCE*, **131**(3), 359-366. https://doi.org/10.1061/(ASCE)1090-0241(2005)131:3(359).

Elam, J. and Björdal, C. (2020), "A review and case studies of factors affecting the stability of wooden foundation piles in urban environments exposed to construction work", *Int. Biodeterioration & Biodegradation*, **148**, 104913. https://doi.org/10.1016/j.ibiod.2020.104913.

Hamza, G. (2012), A numerical study on geotextile stabilized highway embankment under vibration loading.

Hashem, M.D., Abu-Baker, A.M. and Hashem, M.D. (2013), "Numerical modeling of flexible pavement constructed on expansive soils", *Eur. Int. J. Sci. Tech.*, **2**(10), 19-34.

Hyunwook, K. and William, G. (2009), "Finite element cohesive fracture modeling of airport pavements at low temperatures", *Cold Reg. Sci. Technol.*, **57**(2-3), 123-130. https://doi.org/10.1016/j.coldregions.2009.02.004

Lam, S.Y. (2010), "Ground movements due to excavation in clay: physical and analytical models", PhD thesis, University of Cambridge.

Lee, C.J. and Ng, C.W.W. (2004), "Development of downdrag on piles and pile groups in consolidating soil", *J. Geotech. Geoenviron. Eng.*, **130**(9), 905-914. https://doi.org/10.1061/(ASCE)1090-0241(2004)130:9(905).

Mahiyar, H, and Patel, A.N. (1997), "The effect of lateral confinement on the bearing capacity of fine sand", *Indian Geotech. J. New Delhi*, **22**(4), 226-234.

Mayne, P. and Kulhawy, F. (1982), "K0-OCR relationships in soils", *J. Geotech. Eng. - ASCE*, **108**(6), 851-872.

Meyerhof, G.G. (1963), "Some recent research on the bearing capacity of foundations", *Can. Geotech. J.*, **1**(1), 16-26. https://doi.org/10.1139/t63-003.

Ortiz, J.M.R. (2001), "Strengthening of foundations through peripheral confinement", *Proceedings of the 15th the International Conference on Soil Mechanics and Geotechnical Engineering*, Netherlands.

Ottosen, N.S. and Petersson, H. (1992), "Introduction to the finite element method", New York: Prentice Hall.

Rajagopal, K., Krishnaswamy, N. and Latha, G. (1999), "Behavior of sand confined with single and multiple geocells", *Geotext. Geomembranes.*, **17**(3), 171-184. https://doi.org/10.1016/S0266-1144(98)00034-X.

Rashid, A.S.A., Shirazi, M.G., Nazir, R., Mohamad, H., Sahdi, F., and Horpibulsuk, S. (2020), "Bearing capacity performance of soft cohesive soil treated by kenaf limited life geotextile", *Mar. Georesour. Geotec.*, **38**(6), 755-760. https://doi.org/10.1080/1064119X.2019.1616861.

Salencon, J. (2003), "Bearing capacity of strip footings with horizontal confinement", *Comptes Rendus. Mécanique*, **331**(5), 319-324.

Santos de Alencar, A.T., Galindo Aires, R.A. and Melentijevic, S. (2019), "Bearing capacity of foundation on rock mass depending on footing shape and interface roughness", *Geomech. Eng.*, **18**(4), 391-406. https://doi.org/10.12989/gae.2019.18.4.391.

Shirazi, M.G., Rashid, A.S.B.A., Nazir, R.B., Rashid, A.H.B.A., Moayedi, H., Horpibulsuk, S. and Samingthong, W. (2020), "Sustainable soil bearing capacity improvement using natural limited life geotextile reinforcement—A review", *Minerals*, **10**(5), 479. https://doi.org/10.3390/min10050479.

Singh V.K., Prasad, A. and Agrawal, R.K. (2007), "Effect of soil confinement on ultimate bearing capacity of square footing under eccentric inclined load", *Electron. J. Geotech. Eng.*, **12**, 1-14.

Soomro, M.A., Hong, Y., Ng, C.W.W., Lu, H. and Peng, S. (2015), "Load transfer mechanism in pile group due to single tunnel advancement in stiff clay", *Tunn. Undergr. Sp. Tech.*, **45**, 63-72. https://doi.org/10.1016/j.tust.2014.08.001.

Soomro, M.A., Kumar, M., Xiong, H., Mangnejo, D.A. and Mangi, N. (2020), "Investigation of effects of different construction sequences on settlement and load transfer mechanism of single pile due to twin stacked tunnelling", *Tunn. Undergr. Sp. Tech.*, **96**, 103171. https://doi.org/10.1016/j.tust.2019.103171.

Soomro, M.A., Liu, K., Cui, Z.D., Mangi, N. and Mangnejo, D.A. (2024b), "Insights from 3D numerical simulations on the impact of tunnelling on vertical and battered pile groups under lateral loading", *Comput. Geotech.*, **169**, 106195. https://doi.org/10.1016/j.compgeo.2024.106195.

Soomro, M.A., Mangi, N., Cui, Z.D., Liu, K. and Mangnejo, D.A. (2024a), "Evaluation of response mechanisms in an elevated pile group subjected to lateral loading caused by twin-tunnelling", *Comput. Geotech.*, **171**, 106334. https://doi.org/10.1016/j.compgeo.2024.106334.

Soomro, M.A., Mangi, N., Mangnejo, D.A. and Zhang, Z. (2023a), "The responses of battered pile to tunnelling at different depths relative to the pile length", *Geomech. Eng.*, **35**(6), 603-615. https://doi.org/10.12989/gae.2023.35.6.603.

Soomro, M.A., Mangnejo, D.A. and Mangi, N. (2023b), "Investigation of crack growth in a brick masonry wall due to

twin perpendicular excavations", *Geomech. Eng.*, **34**(3), 251-265. https://doi.org/10.12989/gae.2023.34.3.251.

Soomro, M.A., Ng, C.W.W., Liu, K. and Memon, N.A. (2017), "Pile responses to side-by-side twin tunnelling in stiff clay: Effects of different tunnel depths relative to pile", *Comput. Geotech.*, **84**, 101-116. https://doi.org/10.1016/j.compgeo.2016.11.011.

Villalobos, F., Byrne, B.W., Houlsby, G.T. and Martin, C.M. (2003), "Bearing capacity tests of scale suction caisson footings on sand, experimental data", Data report FOT005/1, Civil Engineering Research Group, Department of Engineering Science, The University of Oxford.

Yang, X.L. and Zhang, R. (2017), "Collapse analysis of shallow tunnel subjected to seepage in layered soils considering joined effects of settlement and dilation", *Geomech. Eng*., **13**(2), 217-235. https://doi.org/10.12989/gae.2017.13.2.217.

GC